

UV SENSING EFFECT IN LANGMUIR-BLODGETT COMPLEX FILMS CONTAINING A NOVEL SYNTHESIZED Fe(III) PORPHYRIN

L. BASCHIR^{a,b*}, E. FAGADAR-COSMA^c, I. CREANGA^c, A. PALADE^c,
A. LASCU^c, M. BIRDEANU^d, D. SAVASTRU^a, V. SAVU^a, S. ANTOHE^b,
A. VELEA^e, G. FAGADAR-COSMA^f, M. POPESCU^e, I.D. SIMANDAN^{b,e}

^aNational Institute of Optoelectronics, INOE-2000, 077125 Magurele-Ilfov, Romania

^bUniversity of Bucharest, Faculty of Physics, 077125 Magurele-Ilfov, Romania

^cInstitute of Chemistry Timisoara of Romanian Academy, 300223 Timisoara, Romania

^dNational Institute for Research and Development in Electrochemistry and Condensed Matter, 300224 Timisoara, Romania

^eNational Institute of Materials Physics, 077125 Magurele-Ilfov, Romania

^fPolytechnic University of Timisoara, 300006 Timisoara, Romania

A novel structure of metalloporphyrin, namely: 5,10,15,20-tetrakis(3,4-dimethoxyphenyl)-porphyrin Fe(III) chloride, was successfully synthesized. UV sensitive structure based on barium stearate functionalized with the novel synthesized porphyrin and carbon nanotubes was obtained. A five monolayers structure was deposited from solution by Langmuir – Blodgett technique onto a ceramic substrate with interdigital platinum electrodes. The complex film shows sensitivity to UV radiation due to the fact that an electron is excited from a Fe d orbital into a porphyrin antibonding π orbital and is moved onto the ligand that is attached, facilitating the charge separation, while the presence of SWCNT activates the transport of the charge carriers.

(Received April 1, 2014; Accepted June 13, 2014)

Keywords: Fe(III) porphyrin; Langmuir – Blodgett film; UV sensitive structure; Single wall carbon nanotubes; Sensing effect

1. Introduction

Metalloporphyrins are well-known to play essential functions for life, due to the richness of their optoelectrical properties [1]. Up to date research is focused on synthesizing of novel structures which exhibit properties similar with those of natural porphyrins and on obtaining of thin films of porphyrin derivatives with applications in molecular engineering at different surfaces or interfaces [2, 3]. Some of the well-established methods for preparation of high quality organic thin films are thermal vacuum evaporation especially for small molecules [4, 5], electrochemical polymerization [6], Langmuir - Blodgett (LB) techniques [7] and laser depositions (Pulsed Laser Deposition - PLD and Matrix Assisted Pulsed Laser Evaporation - MAPLE). It is also of great interest to study the topography of porphyrin thin films and the supramolecular architecture of the film, which may influence the performance of the device [8, 9].

The Langmuir – Blodgett is a well-known technique for the preparation of one or several monolayers of organic materials on solid substrates [10]. In the LB technique at the beginning a single layer of amphiphilic molecules is formed on a water surface. One should be very careful when selecting the molecules. A strong anisotropic interaction between the molecules and water should be present in order to ensure that the molecules are bonded to the surface of the water. This

*Corresponding author: baschirlaurentiu@inoe.ro

inhomogenously single molecule layer is then compressed using two barriers which are reducing the area of the water surface and the molecules are packed together. The substrate is then immersed in the liquid. A single monolayer is adsorbed homogeneously with each immersion or emersion step and complex structures are achieved. This technique has successfully used for molecular electronics [11] and to prepare several type of sensors [12 - 16].

Depending on their chirality, single wall carbon nanotubes (SWCNTs) can be metallic, semiconducting, or semi-metallic [17]. These properties can be used for actuators [18], nanoelectronic devices [19] or chemical sensors [20, 21]. The electrical resistance of a semiconducting SWCNTs based sensors exposed gaseous molecules such as NO₂ or NH₃ dramatically increases or decreases at room temperature. The sensor reversibility can be achieved by slow recovery under ambient conditions or by heating at high temperatures. It is of great importance to understand the modification of the resistivity when the nanotubes are in contact with various organic molecules [22].

The present approach is regarding a novel structure of Fe (III) porphyrin with one weak-field monodentate axial ligand coordinated to the iron center, which belongs to neutral five-coordinated species type where Cl is the monodentate anionic axial ligand. Ba stearate was used as amphiphilic molecules and they were functionalized with this novel structure of Fe (III) porphyrin and SWCNT in order to obtain a complex structure sensitive to UV radiation.

Photo-induced charge transfer in carbon nanotubes with linked porphyrin antennae was already reported [23]. The absorption and fluorescence of these complexes show that the carbon nanotubes serve as an efficient electron acceptor, providing a model for the construction of novel photovoltaic devices and light-harvesting systems. The integration of SWCNTs and porphyrins into functional nanohybrids, by means of a combination of associative van der Waals and electrostatic interactions, put into evidence that the SWCNT material acts as an electron acceptor in the system. When the hybrids are irradiated with visible light, a rapid intrahybrid charge separation causes the reduction of the SWCNT and, simultaneously, produces the oxidation of the porphyrin [24]. According to the transient absorption measurements, the radical ion pairs are long-lived, with lifetimes in the microsecond range [25]. Long-lived intracomplex charge separation in polymer-wrapped carbon nanotube–porphyrin was also reported [26].

2. Materials and methods

The bare porphyrin, 5,10,15,20-tetrakis(3,4-dimethoxyphenyl)porphyrin, was synthesized by an Adler-type reaction [27] between pyrrole and 3,4-dimethoxy-benzaldehyde in propionic acid medium, followed by purification by silica gel column chromatography using as eluent chloroform/ethyl ether mixture of ratio 5/1.

The novel metalloporphyrin, 5,10,15,20-tetrakis(3,4-dimethoxy-phenyl)-porphyrin Fe(III) chloride, was obtained by adapted procedure [27] using threefold excess of Iron (III) chloride [28]. The corresponding bare porphyrin (0.312g, 0.36×10^{-3} mol) was dissolved in 240 mL DMF and heated to reflux, under continuous stirring, in a 500 mL flask. To this solution, 0.1777 g FeCl₃ (1.0959×10^{-3} mol) in 20 mL DMF was added dropwise and refluxed for two more hours. The resulted reaction products were dried and the organic component was extracted several times with small quantities of CH₂Cl₂. The organic extracts are put together and three times washed with 5 mL distilled water, then dried on anhydrous Na₂SO₄. The final product is recrystallized from CH₂Cl₂.

Reagents were p.a. grade and were purchased from Fluka, Aldrich and Merck and used as received, excepting pyrrole distilled prior to use. Chloroform was stored over 4Å molecular sieves. CH₂Cl₂ was distilled from CaH₂ under nitrogen. Thin-layer chromatography (TLC) was performed on 25 DC-Alufolien Aluminiumoxid 60 F254 Neutral (Merck). Solvent systems associated with R_f values and chromatography data are reported as v/v ratios.

Column Chromatography was performed at room temperature with silica gel 60 (230-400 mesh, 0.040-0.063 mm), purchased from Merck.

The Fourier Transformed – Infrared Spectroscopy (FT-IR) spectra were carried out, in the 4000-600 cm⁻¹ range on a JASCO 430 FT-IR apparatus, by using KBr pellets. UV-visible spectra

were recorded on a UV/VIS PERKIN ELMER, LAMBDA 12 spectrometer and on a UV-vis JASCO V-650 apparatus. Fluorescence spectra were recorded on a PERKIN ELMER Model LS 55 apparatus in a 1 cm cuvette. Absorption and fluorescence spectra were recorded at ambient temperature using 1 cm path length cells. The emission spectra were recorded with constant slit widths, 7 nm for excitation and 3.5 nm for emission, $\lambda_{ex}=423\text{nm}$. The excitation spectra were recorded with constant slit widths, 15 nm for excitation and 5 nm for emission, $\lambda_{em}=650\text{nm}$.

Atomic force microscopy (AFM) investigations were carried out with a Nanosurf® EasyScan 2 Advanced Research AFM. A stiff ($450\ \mu\text{m} \times 50\ \mu\text{m} \times 2\ \mu\text{m}$) piezoelectric ceramic cantilever (spring constant of $0.2\ \text{Nm}^{-1}$), with an integral tip oscillated near its resonance frequency of about 13 kHz was used in the measurements. AFM measurements were done in ambient conditions (temperature: $21\pm 2\ ^\circ\text{C}$; relative humidity: 50–70%) in contact mode or tapping mode [29].

Ba stearate was functionalized with Fe(III) porphyrin and a mix of metallic (one-third) and semiconducting (two-thirds) SWCNT from Alfa Aesar. Sodium dodecyl benzene sulfonate was used to disperse the carbon nanotubes while benzene was used as a solvent. The mixed solution was stirred at 37 kHz for one hour in order to obtain a good homogeneity [30, 31]. The obtained composition was deposited onto ceramic body with platinum electrodes using a Langmuir – Blodgett KSV 5003 device with a deposition rate of 1mm/min and the pressure chosen for the film transfer was 25 N/m, well above the value corresponding to the beginning of the liquid–solid phase transition. Structures containing five monolayers were obtained. During the deposition all the environmental conditions were monitored.

UV irradiation was carried out with a UV lamp made by Electrotehnica – Bucharest, having the main emission lines in the range of 330-340 nm at a power density of $116\ \mu\text{W}/\text{cm}^2$. The obtained structure was characterized electrically and photo electrically using an experimental setup, containing the UV lamp and a Keithley 2400 Source Measure Unit (SMU). The characterizations were carried out using a $100\ \mu\text{A}$ continuous current injection from a constant current generator thermally insulated and with thermal self-control, developed for this experiment.

3. Results and discussion

The first aim of this study was to obtain a novel structure of iron(III) porphyrin with one weak-field monodentate axial ligand coordinated to the iron center, that belongs to neutral five-coordinated species type (Figure 1) where Cl is the monodentate anionic axial.

The most important analyses results that certify the structure of 5,10,15,20-tetrakis(3,4-dimethoxyphenyl)porphyrin are previously published and given below [32]:

Dark violet solid; yield: 18.4% mp over 320°C ; FT- IR(KBr), cm^{-1} : 762 (γ C-H Ph), 804 (γ C-H Pyrrol), 1022 and 1136 (δ C-H Pyrrol), 1266 (ν C-N), 1461 (ν C=N), 1511 (ν C=C Ph) 1586, 1679 (ν C=C Pyrrol), 2831, 2903 (CH stretching, phenyls groups), 2934, 2985 (γ CH₃aliphatic) 3423 (ν N-H); ¹H-NMR (CDCl₃, 400MHz), d, ppm: -2.70 (brs, 2H, NH), 3.96 (s, 12H, 3-OCH₃), 4.08 (s, 12H, 4-OCH₃), 7.10-7.27 (d, 4H, m-Ph), 7.68-7.71 (d, 4H, o-Ph), 7.78 (s, 4H, o-Ph), 8.90 (s, 8H, β -Pyr); ¹³C-NMR (CDCl₃, 100MHz), d, ppm: 148.85, 147.05, 134.73, 131.12, 130.00, 127.34, 126.75, 119.86, 118.23, 110.22, 109.41, 108.76, 56.08, 55.94; UV-vis, CHCl₃ (λ_{max} (log ϵ): 421.27 (5.49); 518.86 (4.57); 556.38 (4.31); 592.81 (4.05); 649.91 (4.00); TLC (R_f chloroform/dichloroethane/ethyl ether 5/5/1): 0.66; HPLC (RT, min): 3.560; MS (70 eV):m/e= 854 M⁺. (C₅₂O₈N₄H₄₆)⁺. molecular ion). Fluorescence quantum yield $\Phi_f=0.197\pm 0.014$.

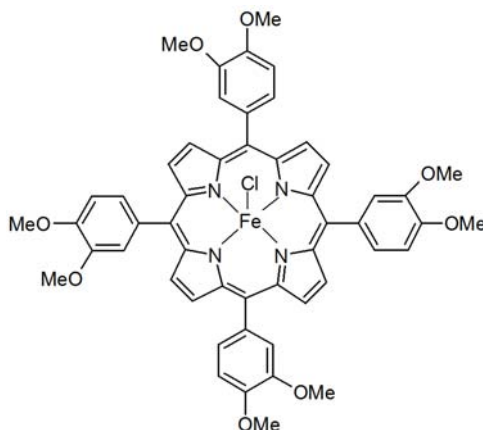


Fig. 1. The structure of 5,10,15,20-tetrakis(3,4-dimethoxyphenyl)-porphyrin Fe(III)

In the FT-IR spectrum of Fe-porphyrin (Figure 2), the absence of N–H stretching vibration in the range $3340\text{--}3423\text{ cm}^{-1}$, which is characteristic of free base porphyrins and also the absence of the out-of-plane N–H deformation bands with peak around 740 cm^{-1} proved that iron was inserted into porphyrin core.

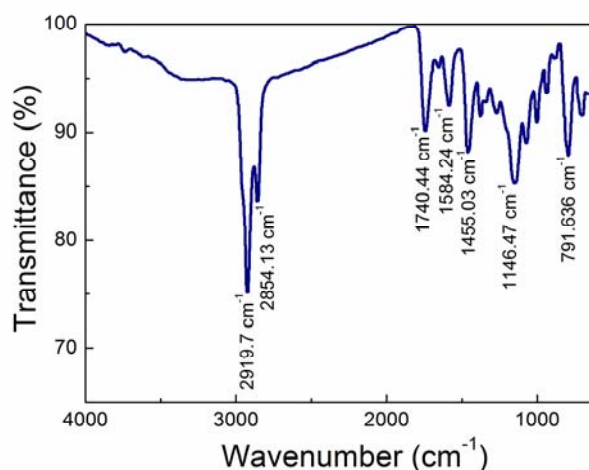


Fig. 2. FT-IR spectrum of 5,10,15,20-tetrakis(3,4-dimethoxyphenyl)-21H,23H-porphyrin Fe(III) chloride

The UV-Visible spectrum in DMF of the free base 5,10,15,20-tetrakis(3,4-dimethoxyphenyl)-21H,23H-porphyrin (Figure 3) is characterized by an intense Soret band at 425.9 nm (B band) and four Q bands of smaller intensity located at 519 nm, 556 nm, 594 nm and 653 nm ($Q_y(1,0)$, $Q_y(0,0)$, $Q_x(1,0)$ and $Q_x(0,0)$, respectively). The B and Q bands are assigned to the $a_{2u} \rightarrow e_g$ and $a_{1u}, a_{2u} \rightarrow e_g$ transitions, respectively.

As comparing to the free porphyrin, the UV-vis spectrum of the corresponding Fe(III) metalloporphyrin presents the Soret band slightly hypsochromically shifted and only one clear Q band at around 571.5 nm (α band). A shoulder at 516 nm (β band) is also represented in the spectrum (Figure 4). According to literature data, high-spin ($S = 5/2$) Fe(III) meso-porphyrin neutral complexes exhibit β and α bands around 513 nm and 570 nm, respectively [33], so that we cannot confirm the spin-state of the central-ion by this method.

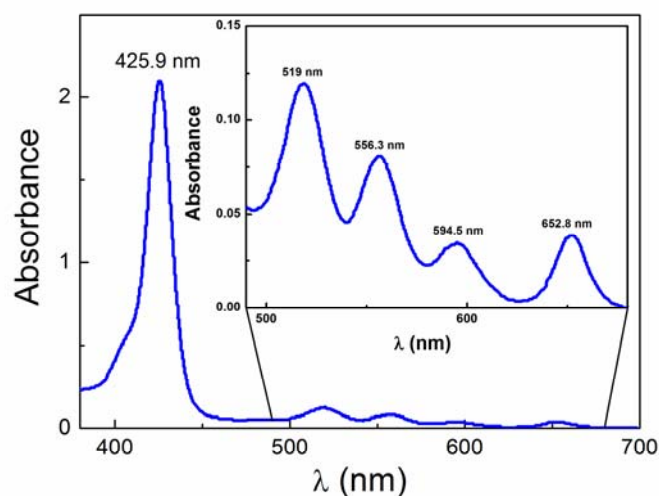


Fig. 3. UV-vis spectrum of *10,15,20-tetrakis(3,4-dimethoxyphenyl)-21H,23H-porphyrin* in DMF solution. In detail Q bands.

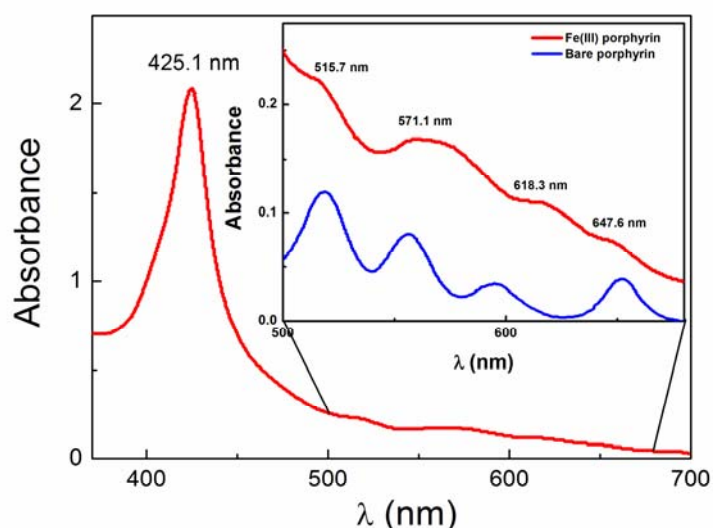


Fig. 4. UV-vis spectrum of *Fe-III-10,15,20-tetrakis(3,4-dimethoxyphenyl) porphyrin chloride* in DMF solution. In detail overlapped Q bands of bare porphyrin and of corresponding *Fe-III-metalloporphyrin*.

The UV-vis spectra of *Fe-III-10,15,20-tetrakis(3,4-dimethoxyphenyl) porphyrin chloride* were performed comparatively in different solvents (Figure 5) in order to estimate the influence of solvent polarity on the shape and location of the main absorption bands. From the overlapped spectra (Figure 5) it can be noticed that the red shift is correlated with the decreasing polarity of solvents, but the shape does not significantly depend on the polarity of the solvent, in good agreement with the behaviour of other reported iron porphyrins [34].

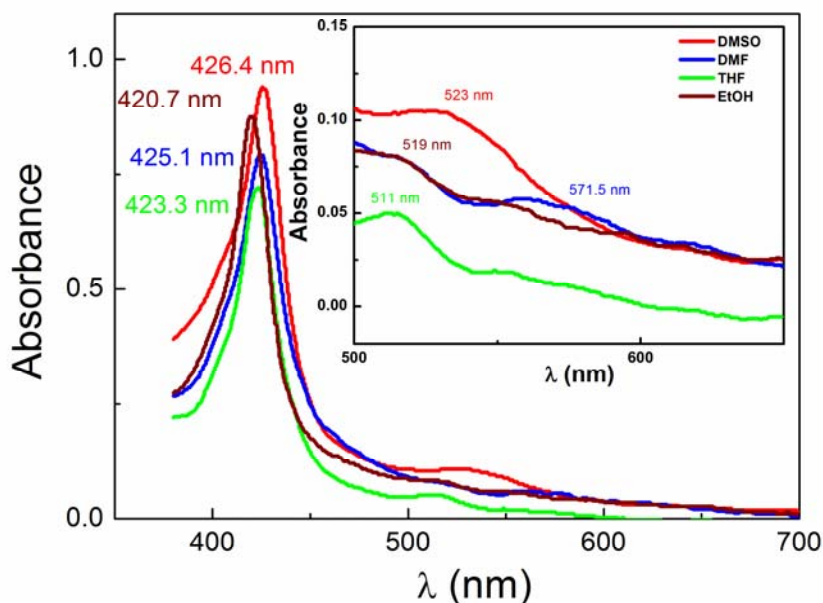


Fig. 5. UV-vis superposed spectra of Fe-III-10,15,20-tetrakis(3,4-dimethoxyphenyl) porphyrin chloride in different solvents: DMSO, DMF, EtOH and THF

A small degree of fluorescence is observed in the emission spectrum of Fe-III-10,15,20-tetrakis(3,4-dimethoxyphenyl) porphyrin chloride (Fig. 6). The Q(0,0) main band is located at 660 nm, whereas the Q(0,1) band of smaller intensity is in the red region at 724 nm. The analogy between the Fe(III)-porphyrin emission spectrum and the spectra of free porphyrins determine our presumption that generation of dimers or oxo-complexes, characteristic of iron porphyrins, might be taken into consideration. Besides that, a small process of demetalation could occur.

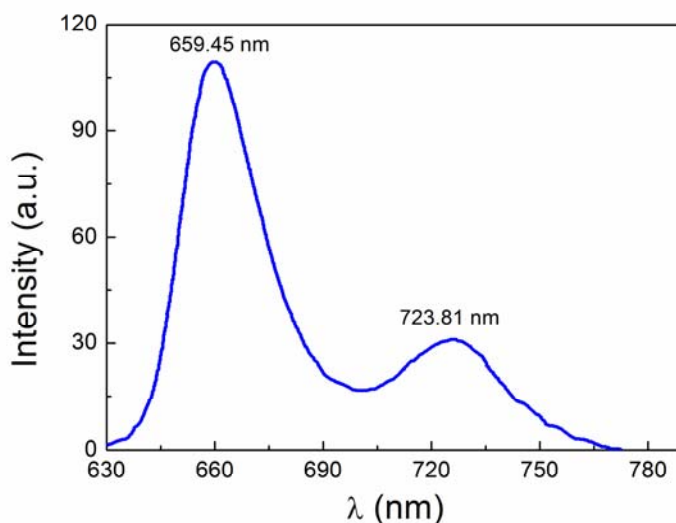


Fig. 6. Fluorescence spectra of Fe-III-10,15,20-tetrakis(3,4-dimethoxyphenyl) porphyrin chloride in DMF, excited at $\lambda_{ex}=423\text{nm}$

Atomic force microscopy analysis was performed to investigate the topography of the surfaces and architecture of the aggregates. Initial triangular H aggregates with dimensions around 70-80 nm (Figure 7 a) are involved in a self-organizing process generating arc structures. Figure 7 b represents 3D tapping mode AFM image of a discontinuous ring organization of the aggregates with internal diameters from 400 to 900 nm. Porphyrins are known to generate triangular H aggregates that are able to agglomerate by the J-aggregation lateral packing mechanism and to form rings by hydrogen bonding.

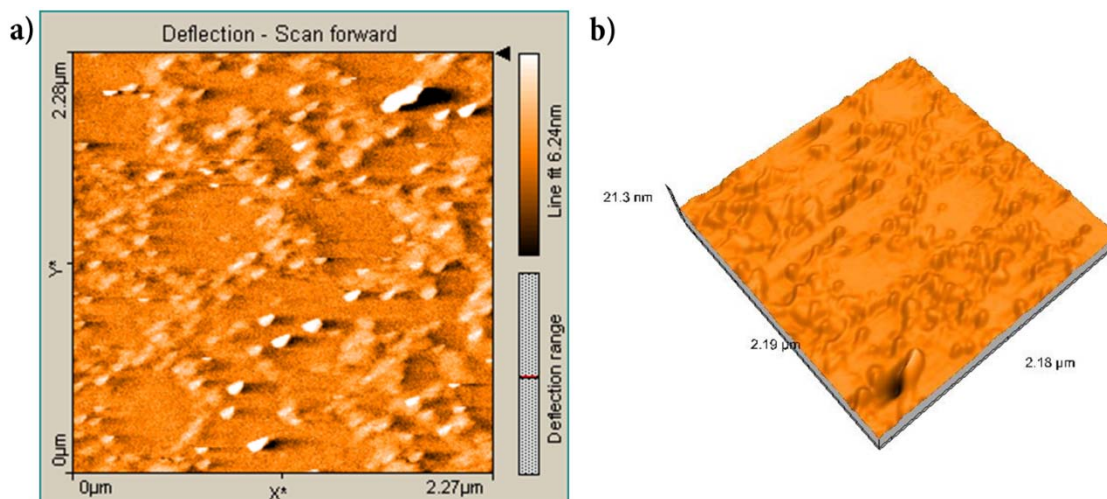


Fig. 7. a) 2D AFM Image in contact mode of Fe-III-10,15,20-tetrakis(3,4-dimethoxyphenyl) porphyrin b) 3D tapping mode AFM image of a ring organization of the Fe –porphyrin

The response to the continuous UV radiation for 1200 seconds of the 5 Langmuir Blodgett monolayers sensitive structure based on Fe – porphyrin is represented in Figure 8.

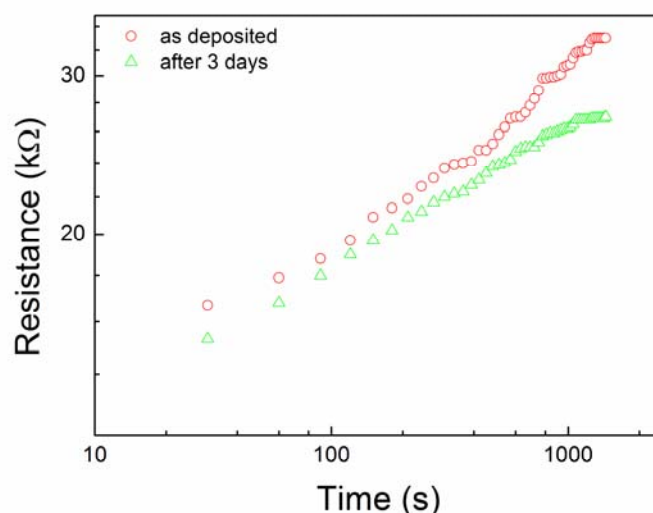


Fig. 8. The effect of UV radiation of 5 Langmuir Blodgett (5LB) monolayers structures based on Fe –porphyrin. (as deposited – red circles, after 3 days – green triangles)

As we can see from Figure 8, during the UV irradiation of the prepared structures carrying a continuous current of $100\mu\text{A}$, their electrical resistance increases about linearly with the same slope in both the cases: as deposited and after 3 days of irradiation. The decreasing of the electrical

resistance in time, in the dark, could be explained as a heating effect associated with the injected current. Taking into account that Ba stearate was functionalized with Fe(III) porphyrin and a mix of metallic and semiconducting SWCNT, it is possible that the presence of relatively large concentration of metallic component of SWCNT to induce a metallic behavior of resistance-temperature dependence. After the 3 days the samples are very well dried and then their resistances were decreased. A situation like this one appears also at illumination, when the non-equilibrium charge carriers will be involved in the charge transport mechanisms, decreasing the resistance.

When the UV irradiation is stopped an instant rise of 2 to 3 k Ω in electrical resistance occurs (Figure 9). Normally, from physical point of view, when the light is turned off, the photo-generation of the non-equilibrium charge carriers disappears, the electrical resistance increasing again to its value corresponding to the dark state. If the sensor is UV illuminated again, the resistance returns to its dynamic value following the previous trend. Taking into account the periodicity of this signal we can talk on the presence of a structure sensitive to UV irradiation which behaves as a sensor able to detect UV radiation by the jump in the electrical resistance of about 2-3 k Ω with a time constant of about 5-6 minutes, see the Figure 10.

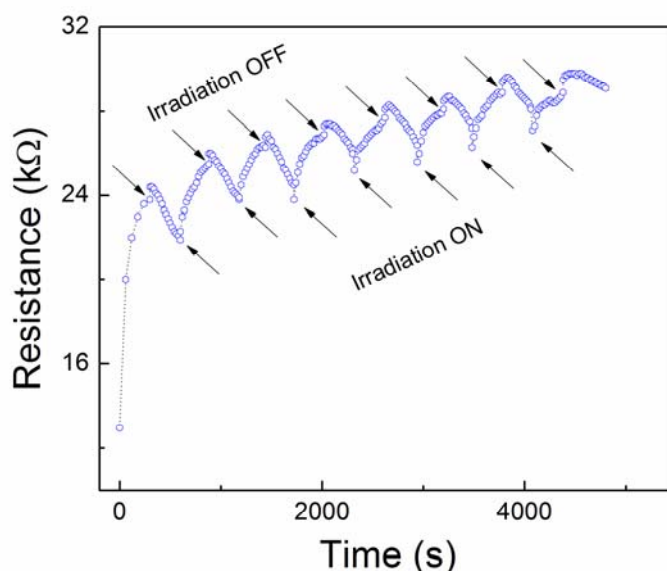


Fig. 9. The effect of UV radiation (ON and OFF) of 5 Langmuir Blodgett thin layers structures based on Fe-porphyrin.

It is well known that successful porphyrins exhibit a push-pull nature in the transition from ground state to excited state. In the peculiar case of our iron-metalloporphyrin structure we presume that an electron is excited from a Fe d orbital into a porphyrin antibonding π orbital and is moved onto the ligand facilitating the charge separation. As a general rule regarding porphyrins, the HOMO has to reside on the donor while the LUMO resides on the acceptor side. This type of push pull excitation [35], increases the rate of photo-generation of non-equilibrium charge carrier, which coupled with activation of charge transport induced by the presence of SWNTs give rise to the above behavior of the prepared structures.

Based on the knowledge in NLO and switching studies [36], focused on a A4 symmetric porphyrin possessing methoxy groups at the phenyl ring, especially chosen for their donating abilities, we decided to synthesize a di-methoxy substituted porphyrin structure Fe (III) complexed, linked with a strong electronegative axial ligand, presuming to produce enhancement of NLO. Coordination of a metal ion by porphyrins is always accompanied by an enhanced nonlinearity due to better conjugation.

Improved optical nonlinear behavior is expected from supramolecular donor-acceptor systems of carbon nanotubes (CNTs) or single-walled nanotubes (SWNTs) with planar aromatic

porphyrins with an additional scattering component expected to enhance the nonlinear optical limiting behavior of the bare porphyrin macrocycle improving also the oxygen sensing capabilities of photosensitizers (Fig 10).

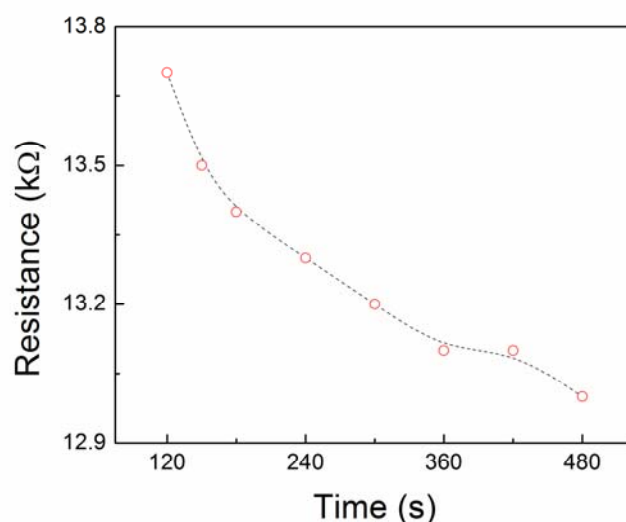


Fig. 10. The effect of O_2 ionization on the behavior of 5 Langmuir Blodgett thin layers structures based on Fe-porphyrin at room conditions.

In the electron excitation process, the significant conjugation of the π levels of both the porphyrin and linker facilitates a charge transfer from the occupied π levels of the porphyrin core, to the antibonding π^* orbitals of the linker carrying the push-pull phenomenon. The change in dipole moment indicates that the chromophores polarizability along the donor-acceptor axis can be further enhance by metal to macrocycle charge transfer [37].

On the other hand the hyperpolarizability is dependent on the type of aggregate formed. Thus, compared to the monomers, formation of J-aggregation, as reported in our case, resulted in doubling of the β tensor values [38].

4. Conclusions

A new structure of iron(III) porphyrin with one weak-field monodentate axial ligand coordinated to the iron center where Cl is the monodentate anionic axial was successfully prepared. The FT-IR spectrum of Fe-porphyrin proved that iron was inserted into the porphyrin core but the spin-state of the central-ion cannot be confirmed. The UV-vis spectrum is characterized by an intense Soret band at 425.9 nm (B band) and four Q bands of smaller intensity located at 519 nm, 556 nm, and 594 nm. A small degree of fluorescence was observed in the emission spectrum of Fe-III-10,15,20-tetrakis(3,4-dimethoxyphenyl) porphyrin chloride with the main band located at 660 nm.

A sensitive structure based on Ba stearate functionalized with 5,10,15,20-tetrakis(3,4-dimethoxy-phenyl)-porphyrin Fe(III) chloride and carbon nanotubes had been successfully developed. This structure deposited on a ceramic substrate with platinum interdigital electrodes showed a strong sensibility to UV irradiation. This could be due to the excitation of the electrons from the Fe d orbitals into porphyrin antibonding π orbitals which facilitates the charge photo-generation coupled with activation of charge transport induced by the presence of SWNTs.

Acknowledgements

This paper was supported by the Sectorial Operational Programme Human Resources Development (SOP HRD), financed from the European Social Fund and by the Romanian Government under the contract number SOP HRD/107/1.5/S/82514, for which L. Baschir is grateful. Authors from Institute of Chemistry Timisoara of Romanian Academy are kindly acknowledging Programme 2 and Project STAR-SAFEAIR/76/2013.

References

- [1] E. Fagadar-Cosma, L. Cseh, V. Badea, G. Fagadar-Cosma, D. Vlascici, *Comb. Chem. High T. Scr.* **10**, 466 (2007).
- [2] M. T. Oztek, M.D. Hampton, D.K. Slattery, S. Loucks, *Int. J. Hydrogen Energ.* **36**, 6705 (2011).
- [3] L. Lvova, C. Di Natale, R. Paolesse, *Sensor. Actuat. B-Chem.* **179**, 21 (2013)
- [4] S. Antohe, L. Tugulea, *Phys. Status Solidi A* **128**, 253 (1991) -260
- [5] S. Antohe, *Phys. Status Solidi A* **136**, 401 (1993).
- [6] F. Armijo, M. C. Goya, Y. Gimeno, M. C. Arevalo, M. J. Aguirre, A. H. Creus, *Electrochem. Commun.* **8**, 779 (2006)
- [7] M. Popescu, I.D. Simandan, F. Sava, A. Velea, E. Fagadar-Cosma, *Dig. J. Nanomater. Bios.* **6**(3), 1253 (2011).
- [8] E. Fagadar-Cosma, G. Fagadar-Cosma, M. Vasile, C. Enache, *Curr. Org. Chem.* **16**, 931 (2012).
- [9] D. Skrzypek, I. Madejska, J. Habdas, A. Dudkowiak, *J. Molec. Struct.* **876**, 177 (2008).
- [10] I. R. Peterson, *Langmuir Blodgett Films*, *J. Phys. D* **23**(4), 379 (1990).
- [11] S. A. Hussain, *Langmuir-Blodgett Films a unique tool for molecular electronics* arXiv:0908.1814 (2009) 1.
- [12] R. Singhal, A. Chaubey, K. Kaneto, W. Takashima, B. D. Malhotra, *Biotechnol. Bioeng.* **85**(3), 277 (2004).
- [13] I. D. Simandan, F. Sava, A. Velea, A. Lorinczi, M. Popescu, *Optoelectron. Adv. Mater. – Rapid Commun.* **4**(8), 1178 (2010).
- [14] S. B. Ogale, P.G. Bilurkar, N. Mate, S. M. Kanetkar, N. Parikh, B. Patnaik, *J. Appl. Phys.* **72**, 3765 (1992)
- [15] C.J. Brabec, V. Dyakonov, J. Parisi, N.S. Sariciftci, *Organic Photovoltaics: Concepts and Realization*; Vol. 60, Berlin, 2003.
- [16] I. D. Simandan, M. Popescu, A. Lorinczi, A. Velea, E. Fagadar-Cosma, *Dig. J. Nanomater. and Bios.* **5**(4), 1029 (2010).
- [17] M. S. Dresselhaus, G. Dresselhaus, P. C. Eklund, *Science of Fullerenes and Carbon Nanotubes*, Academic Press, San Diego, 1996.
- [18] R. H. Baughman, C. Cui, A. A. Zakhidov, Z. Iqbal, J. N. Barisci, G. M. Spinks, G. G. Wallace, A. Mazzoldi, D. De Rossi, A. G. Rinzler, O. Jaschinski, S. Roth, M. Kertesz, *Carbon Nanotube Actuators*, *Science* **284**, 1340 (1999).
- [19] S. Tans, A. Verschueren, C. Dekker, *Nature* **393**, 49 (1998).
- [20] G. U. Sumanasekera, B. K. Pradhan, C. K. W. Adu, R. E. Romero, P. C. Eklund, *Prepr. Pap.-Am. Chem. Soc., Div. Fuel Chem.* **49**(2), 885 (2004).
- [21] W.-D. Zhang, W.-H. Zhang, *Carbon Nanotubes as Active Components for Gas Sensors*, *J. Sens.* (2009), 160698
- [22] J. Kong, N. R. Franklin, C. Zhou, M. G. Chapline, S. Peng, K. Cho, H. Dai, *Nanotube Molecular Wires as Chemical Sensors*, *Science* **287**, 622 (2000).
- [23] D. Baskaran, J. W. Mays, X. P. Zhang, M. S. Bratcher, *J. Am. Chem. Soc.*, **127**, 6916 (2005).
- [24] D. M. Guldi, G. M. A. Rahman, M. Prato, N. Jux, S. Qin, W. Ford, *Angew. Chem., Int. Ed.*, **44**, 2015 (2005) .
- [25] D. M. Guldi, G.M. Aminur Rahman, N. Jux, D. Balbinot, U. Hartnagel, N. Tagmatarchis, M. Prato, *J. Am. Chem. Soc.*, **127**, 9830 (2005).

- [26] D. M. Guldi, H. Taieb, G.M. Aminur Rahman, N. Tagmatarchis, M. Prato, *Adv. Mater.* **17**, 871 (2005).
- [27] A. D. Adler, F.R. Longo, J. D. Finarelli, J. Goldmacher, J. Assour, L. Korsakoff, *J. Org. Chem.* **32**, 476 (1967).
- [28] D. Skrzypek, I. Madejska, J. Habdas, A. Dudkowiak, *J. Mol. Struct.* **876**, 177 (2008)
- [29] E. Fagadar-Cosma, C. Enache, I. Armeanu, D. Dascalu, G. Fagadar-Cosma, M. Vasile, I. Grozescu, *Mater. Res. Bull.* **44**, 426 (2009).
- [30] L. Baschir, M. Popescu, S. Antohe, *Journal of Ovonic Res.* **8**(6), 189 (2012).
- [31] L. Baschir, S. Antohe, A.Radu, R. Constantineanu, S. Iftimie, I. D. Simandan, M. Popescu *Dig. J. Nanomater. Bios.* **8**(4) 1645 (2013)
- [32] E. Fagadar-Cosma, C. Enache, D. Vlascici, G. Fagadar-Cosma, M. Vasile, G. Bazylak, *Mater. Res. Bull.* **44**, 2186 (2009).
- [33] M. Dhifet, M. S. Belkhiria, M. Giorgi, H. NasriInorg. *Chim. Acta* **362**, 2776 (2009)
- [34] M. Makarska-Bialokoz, G. Pratviel, St. Radzki, *J. Mol. Struct.* **875**, 468 (2008)
- [35] R. Ma, P. Guo, H. Cui, X. Zhang, M. K. Nazeeruddin, M. Gratzel, *J. Phys. Chem. A* **113**, 10119 (2009).
- [36] Mathias O. Senge, Marijana Fazekas, Eleni G. A. Notaras, Werner J. Blau, Monika Zawadzka, Oliver B. Locos, Eimhin M. Ni Mhuirheartaigh, *Adv. Mater.* **19**, 2737 (2007)
- [37] Z. S. Yoon, J. H. Kwon, M.-C. Yoon, M. K. Koh, S. B. Noh, J. L. Sessler, J. T. Lee, D. Seidel, A. Aguilar, S. Shimizu, M. Suzuki, A. Osuka, D. Kim, *J. Am. Chem. Soc.* **128**, 14128 (2006)
- [38] P. C. Ray, J. Leszczynski, *Chem. Phys. Lett.* **419**, 578 (2006).